Characterisation of iron tetraarylporphyrins co-ordinatively bound to solid supports

Paul R. Cooke, Claire Gilmartin, Gary W. Gray and John R. Lindsay Smith *
Department of Chemistry, University of York, York, UK YO1 5DD

Iron(III) tetra(pentafluorophenyl)- and tetra(2,6-dichlorophenyl)-porphyrin (FeTPFPP and FeTDCPP) have been co-ordinatively bound to imidazole and pyridine groups on organic polymers (PSIm and PVP) and on the surface of silica (SiIm and SiPy). The oxidation and spin states of the resulting supported catalysts have been characterised by UV–VIS, resonance Raman and EPR spectroscopy. Evidence is presented that the iron porphyrins on the flexible organic polymers are all low-spin *bis*-ligated iron(II) species. In contrast, on the rigid modified silicas the iron porphyrins are mono-ligated and high spin. Furthermore whereas FeTDCPP on SiIm is an iron(III) species, on SiPy it is iron(II) and FeTPFPP on SiIm is a mixture of both oxidation states.

Supported metalloporphyrins have been widely studied as models for haem protein oxygen carriers (haemoglobin and myoglobin) and oxidation catalysts (peroxidases, catalases and cytochrome P450).[1] Despite this interest and the potential industrial applications of some of these systems, there have been surprisingly few studies on the characterisation of supported metalloporphyrins. By contrast metalloporphyrins in homogeneous solution have been extensively studied with a range of techniques (EPR,[2] IR,[3] mössbauer,[4] NMR,[5] resonance Raman,[6] UV–VIS[7] and X-ray absorption[8] spectroscopy and electrochemical methods[9]).

Anchoring metalloporphyrins to solid supports can have a marked influence on the chemistry of these systems. The support provides the local environment of the reaction and can lead to catalyst site-isolation. Other obvious advantages of such systems can include ease of separation from products and improved catalyst stability, recovery and re-use. Without evidence to the contrary, it is generally assumed that the chemistry of a supported catalyst in a heterogeneous system is the same as that of the corresponding catalyst in homogeneous solution.

Our recent studies on alkene epoxidation, using iron tetraarylporphyrins co-ordinatively bound to ligands on the surface of organic polymers and inorganic solids, have revealed significant differences in appearance, properties and reactivity of a given metalloporphyrin–ligand pair on organic polymers and inorganic supports.[10] Thus FeTPFPP and FeTDCPP† are strongly bound to the organic polymers, PSIm and PVP, and give red–orange coloured materials, whereas with the modified silicas, SiIm and SiPy, the catalysts have a brown appearance and the metalloporphyrin is more readily leached off by solvents, such as methanol, which can act as a competitive ligand. These differences we attributed to the ability of the flexible polymer supports to form *bis*-ligated complexes (Fig. 1) which are not possible with the rigid inorganic solids (Fig. 2). Indeed the colours of the polymer supported catalysts closely resemble those of solutions of the *bis*-imidazole and *bis*-pyridine complexes of FeTPFPP and FeTDCPP.

With the intention of obtaining more information on the support–iron porphyrin interactions, we have attempted to characterise the spin and oxidation states of the metals in the supported-catalysts. This paper reports the results from these studies.

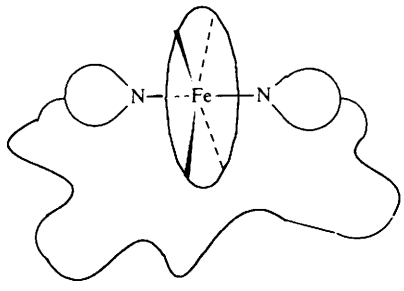

Fig. 1 Schematic diagram of an iron porphyrin supported on PSIm or PVP

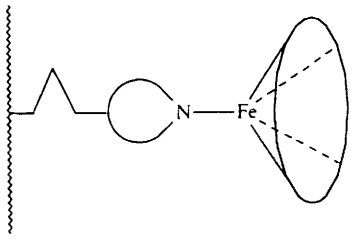

Fig. 2 Schematic diagram of an iron porphyrin supported on silica modified with imidazole or pyridine groups

Results and discussion

This study is restricted to two iron porphyrins (FeTPFPP and FeTDCPP) and two nitrogen ligands, imidazole and pyridine, covalently bound by their 1- and 4-positions respectively to organic polymers (PSIm and PVP) and to surface modified silica (SiIm and SiPy).[10] In the latter materials the organic ligand is attached by 1,3-silylpropyl and 1,4-silylbutyl linkers respectively. Two of the most robust of these supported metalloporphyrins (SiIm–FeTDCPP and SiPy–FeTDCPP)

† Abbreviations: PSIm, *N*-imidazylmethylated polystyrene; PVP, poly(4-vinylpyridine); SiIm, imidazole modified silica; SiPy, pyridine modified silica; porphyrin ligands; TPP, tetraphenyl; TPFPP, tetra(pentafluorophenyl); TDCPP, tetra(2,6-dichlorophenyl); T4MPyP, tetra(4-*N*-methylpyridyl).

have been investigated in detail as catalysts for epoxidation of alkenes.[10]

The amounts of nitrogen base on each support have been obtained from elemental analysis and used to calculate the extent of support modification (Table 1). These materials have then been loaded with the two iron(III) porphyrins by stirring dichloromethane or methanol solutions of Fe^{III}TPFPP or Fe^{III}TDCPP with suspensions of the support. UV–VIS determination of the non-loaded metalloporphyrin gave the extent of loading and from this the excess of ligand over metalloporphyrin for each supported catalyst (Table 1). The resistance to leaching, and efficiency and stability of these catalysts in alkene epoxidation has been reported.[10]

SEM measurements on the silica supported catalysts, at magnifications of 300, 5000 and 30 000, reveal that support surface modification and iron porphyrin loading do not lead to any gross structural changes to these materials.

None of the above measurements provides information on the supported catalysts at the molecular level. To obtain such information we have used a selection of spectroscopic methods.

IR and CPMAS ^{13}C NMR spectroscopy

Qualitative information about the ligand and the linker units on the modified silicas, but not of the organic polymers, can be obtained from IR and CPMAS ^{13}C NMR spectroscopy. IR and diffuse reflectance FTIR spectroscopy show the presence of the alkyl chain and nitrogen ligands on the modified silicas, however, the absorbances from the organic groups are very small compared with those from the silica support and provide little structural information.[10] By contrast, although the peaks in the CPMAS ^{13}C NMR spectra of the modified supports are broader than those from the homogeneous solution analogues (4-ethylpyridine and *N*-methylimidazole) they clearly identify the covalently bound pyridine and imidazole groups (Table 2). The low loadings of iron porphyrins precludes these latter two methods from being used to study the supported macrocycles.

Table 1 Support loadings of co-ordinatively bound FeTPFPP and FeTDCPP

Supported porphyrin	Loading		Ratio of ligand to porphyrin[c]
	Ligand[a]	Porphyrin[b]	
PSIm–FeTPFPP	4.1	10	420
PSIm–FeTDCPP	4.1	10	390
PVP–FeTPFPP	8.9	8	1080
PVP–FeTDCPP	8.9	10	840
SiIm–FeTPFPP	1.3	6	210
SiIm–FeTDCPP	1.3	4	310
SiPy–FeTPFPP	0.8	6	140
SiPy–FeTDCPP	0.8	4	140

[a] mmol g^{-1} of imidazole or pyridine. [b] mg g^{-1} after washing with CH_2Cl_2 and MeOH. [c] Molar ratio of ligand to metalloporphyrin.

Furthermore the paramagnetic effects of the iron in the NMR spectra of iron(III) porphyrins observed in solution were not detected with the supported materials.

UV–VIS Spectroscopy of supported catalysts

Three methods were used to measure the UV–VIS spectra of the supported catalysts. Routinely spectra were recorded of nujol mulls[12] and of suspensions in dichloromethane (see Fig. 3). (The latter required the use of a diode array spectrometer.) One of the catalysts (SiPy–FeTDCPP) was also examined by diffuse reflectance UV–VIS spectroscopy. The spectra of the mulls and suspensions contained some extraneous peaks and the intensity of the porphyrin absorptions were lower than those from analogous homogeneous systems. Consequently although the Soret peaks were clearly visible (Table 3), the λ_{max} values of the less intense α and β bands, between 500 and 700 nm, could not always be reliably assigned. For the iron porphyrins on polymer supports it was usually easier to obtain a UV–VIS spectrum by the mull method, unless the particles were very finely ground, since the low density of the materials made the formation of suspensions difficult. Lower density solvents (hexane, methanol and toluene) were investigated but with these the solid precipitated too rapidly to measure UV–VIS spectra.

To help characterise the supported FeTPFPP and FeTDCPP, solution models were first investigated. *N*-Methylimidazole was used as a model for SiIm, *N*-benzylimidazole for PSIm and 4-methylpyridine for PVP and SiPy. The UV–VIS spectra of solutions of FeTPFPP and FeTDCPP in the presence and absence of these nitrogen ligands were recorded.

UV–VIS spectroscopy of iron porphyrins provides information on the spin and oxidation state of the iron atom from the Soret peak (typically near 400 nm) and the less intense α and β

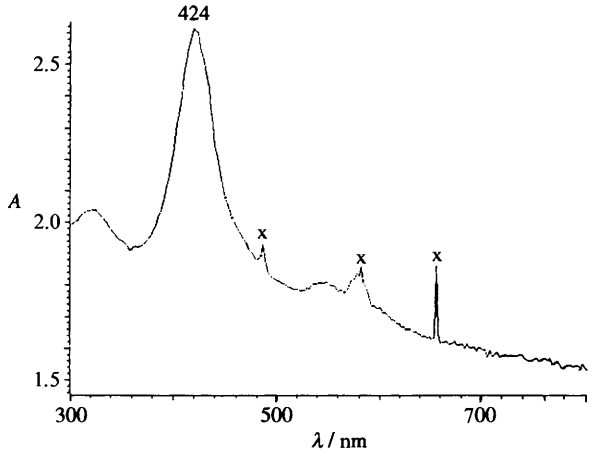

Fig. 3 UV–VIS spectrum of SiIm–FeTDCPP suspended in $CHCl_3$; X, extraneous peaks from support

Table 2 CPMAS ^{13}C NMR δ values for pyridine and imidazole modified silica and comparable values for solutions of *N*-methylimidazole and 4-ethylpyridine

Nitrogen ligand	$\delta_{^{13}C}$					
	Alkyl chain	Methoxysilyl	Heterocycle			
			C-2	C-3	C-4	C-5
SiIm	0–30	49	137	—	117	126
N-Methylimidazole[a]	33		138	—	120	129
SiPy	0–30	50	148	123	nd[b]	
4-Ethylpyridine[c]	13 (CH_3) 27 (CH_2)		149	122	151	

[a] Deuteriochloroform solution. [b] Not detected. [c] From ref. 11.

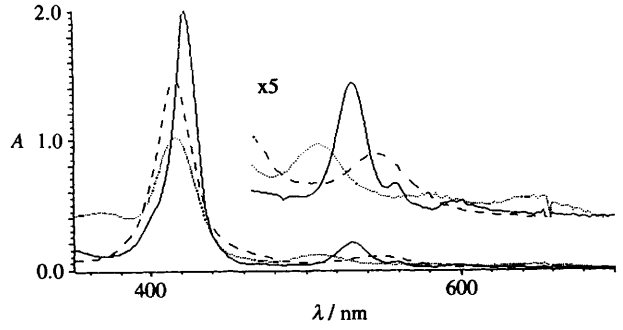

Fig. 4 UV–VIS spectrum of $Fe^{III}TDCPP$ in CH_2Cl_2 (· · ·), in the presence of 400-fold excess of *N*-benzylimidazole (– – –), in the presence of excess of NH_2NH_2 (——)

Table 3 λ_{max} values of Soret peaks in UV–VIS spectra and resonance Raman data of supported FeTPFPP and FeTDCPP

Porphyrin	Support	Soret λ_{max}/nm (Method)[a]	Resonance Raman Band A/cm^{-1}	Band D/cm^{-1}
FeTPFPP	PSIm	432 (s)	1354	1566
FeTPFPP	PVP	418 (s)		
FeTPFPP	SiIm	416 (s)	1364 (major) 1345 (minor)	nd[b]
FeTPFPP	SiPy	418 (s)		
FeTDCPP	PSIm	430 (s)		
FeTDCPP	PVP	430 (m)	1353	1558
FeTDCPP	SiIm	424 (s) 420 (m)	1362	nd[b]
FeTDCPP	SiPy	428 (s) 424 (m) 421 (d)	1353	1555

[a] m, Nujol mull; s, suspension in CH_2Cl_2 and d, diffuse reflectance. [b] Not detected.

bands (between 500 and 700 nm). In the presence of excess of the ligands two changes occurred in the UV–VIS spectra of the iron(III) porphyrins. First, they led to the conversion of the complexes from high-spin (pentaco-ordinate) to low-spin (hexaco-ordinate) *bis*-ligated iron(III) porphyrins. Although the spin change of the iron(III) does not bring about a shift of the λ_{max} of the Soret peak, a characteristic change in α and β bands is observed (Fig. 4 and Table 4).[13] It is well documented that the addition of nitrogen bases, such as imidazole or *N*-substituted imidazoles, to solutions of high-spin iron(III) porphyrins leads to the formation of *bis*-ligated, low-spin iron(III) complexes[9b,13,14] which is accompanied by the replacement of the two or three peaks between 500 and 700 nm, characteristic of the high-spin iron(III), by a single absorption at *ca.* 550 nm.[13] Secondly, with some of the ligands, particularly in the absence of air, reduction to a low-spin *bis*-ligated iron(II) porphyrin occurred. Low-spin iron(II) complexes have a red shifted Soret peak and two characteristic peaks at longer wavelength (between 500 and 700 nm)[15] (Fig. 5 and Table 4). Of the three nitrogen ligands examined, their effectiveness as reducing agents increases in the order NMeIm < NBzIm ≪ 4MePy. Furthermore FeTPFPP undergoes reduction more readily than FeTDCPP. Thus a 400-fold excess of *N*-methylimidazole in dichloromethane converted both iron(III) porphyrins to the corresponding low-spin iron(III) complexes. Prolonged reaction (24 h) in the absence of air led to the partial reduction of FeTPFPP but not of FeTDCPP. Likewise with *N*-benzylimidazole (a model for PSIm) FeTDCPP gave low-spin $Fe^{III}TDCPP(NBzIm)_2$ whereas FeTPFPP gave a spectrum corresponding to a mixture

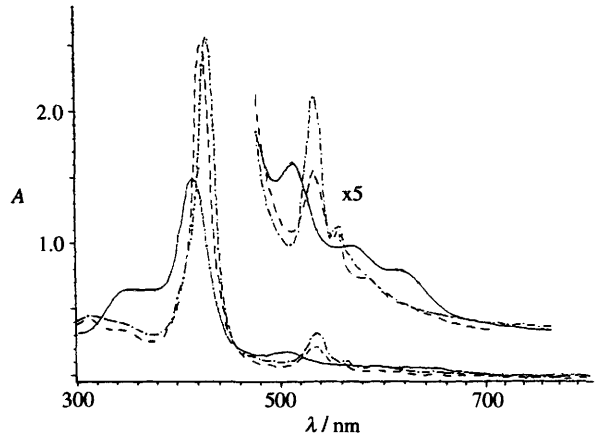

Fig. 5 UV–VIS spectrum of $Fe^{III}TDCPP$ in $CHCl_3$ (——), in the presence of 400-fold excess of 4-methylpyridine (– – – –), after reduction to $Fe^{II}TDCPP$ with sodium dithionite (– · · · –)

Table 4 λ_{max} values of iron(III) and iron(II) complexes of TPFPP and TDCPP in dichloromethane

Iron porphyrin	Spin state[a]	λ_{max}/nm				
$Fe^{III}TPFPP(Cl)$	HS	350	412	504	630	
$Fe^{III}TDCPP(Cl)$	HS	366	416	508	580	648
$Fe^{III}TPFPP(NMeIm)_2$[b]	LS	326	412	538		
$Fe^{III}TDCPP(NBzIm)_2$[b]	LS	324	416	550		
$Fe^{II}TPFPP(NH_2NH_2)_2$[c]	LS		420	526	552	
$Fe^{II}TDCPP(NH_2NH_2)_2$[c]	LS	314	424	530	558	
$Fe^{II}TDCPP(2MeIm)$[b]	HS	340	424	570		

[a] HS, high spin; LS, low spin. [b] 400-fold excess of nitrogen ligand over iron porphyrin. [c] Reduction with an excess of hydrazine.

of low-spin complexes of iron(III) and iron(II). 4-Methylpyridine in the absence of air led to the complete reduction of both iron(III) porphyrins. Spectra of authentic low-spin iron(II) porphyrins were readily obtained using hydrazine as the reductant. High-spin $Fe^{II}TDCPP$ was prepared by adding a 400-fold excess of 2-methylimidazole to a solution of $Fe^{II}TDCPP$[16] (Table 4). Thus depending on the iron porphyrin and reaction conditions, the initial high-spin iron(III) complex was converted by the excess of the nitrogen ligand to the expected low-spin species which was then in some reactions fully or partially reduced to the corresponding low-spin iron(II) porphyrin. These results indicate that it is not safe to assume that the co-ordinatively supported porphyrins are all iron(III) complexes. Their spin and oxidation states need to be assigned.

Walker and her co-workers[13] have shown that *ortho*-chloro groups do not prevent the binding of *N*-substituted imidazoles to FeTDCPP and La Mar and his co-workers[14c] reported that electron releasing substituents on the *meso*-aryl groups of iron(III) tetraarylporphyrins increase the equilibrium constant for *bis*-ligation. Hence it is likely that FeTDCPP ligates the nitrogenous bases more strongly than FeTPFPP. In contrast, the strongly electron-withdrawing pentafluorophenyl groups of TPFPP will favour the reduction of iron(III) to iron(II) by comparison with TDCPP.[9b] β-Pyrrole halogenated analogues of FeTPFPP and FeTDCPP show an even greater tendency to form iron(II) species.[17]

There have been a number of studies of the reduction of iron(III) porphyrins, in particular of FeTPP, by nitrogen bases such as piperidine and pyridine. The reaction mechanisms and the nature of the amine oxidation products remain uncertain,[18] however, it is generally accepted that reduction is an inner-sphere process that involves electron-transfer to the axially ligated nitrogen base. In agreement with this conclusion we have

found that the sterically hindered 2-methylpyridine and 2,4,6-trimethylpyridine do not ligate with FeTPFPP or FeTDCPP or bring about their reduction.[17] Furthermore the faster reduction in benzene compared with dichloromethane can be rationalised by considering *bis*-ligation of nitrogen bases to iron(III) porphyrins to form a charged $Fe^{III}P(B)_2^+ Cl^-$ ion-pair (where B represents the nitrogenous base)[14c] occurs prior to reduction to neutral $Fe^{II}P(B)_2$. The latter process would be less favourable in the more polar dichloromethane which would stabilise the ion-pair better than benzene.

Of the solution models for the supported ligands, 4-methylpyridine is the best reducing agent and an excess of this base in effect leads to the complete reduction of both iron(III) porphyrins even in the presence of air. Comparison of the λ_{max} values of the Soret peaks of the UV–VIS spectra of these solutions with those of the catalysts supported on PVP and SiPy, the supported analogues of 4-methylpyridine, suggests that both metalloporphyrins are bound as iron(II) complexes. Since PVP is a flexible polymer, it is likely as suggested previously[10a] that with this support the complexes are *bis*-ligated low-spin species. However, with SiPy, the 4-methylpyridyl groups are attached to a rigid support by a short linker and it is most unlikely that they will be able to *bis*-ligate to the iron porphyrins. Consequently the iron(II) species are either mixed ligand (H_2O, SiPy) hexaco-ordinated or mono-ligated pentaco-ordinated high spin complexes in which the iron atom is displaced from the plane of the porphyrin ring (Fig. 2). In agreement with the latter conclusion the λ_{max} of the Soret peak of high-spin iron(II) TDCPP(2MeIm) is the same as that of its low-spin analogue showing an 8 nm red shift from that of high-spin iron(III) TDCPP. This is somewhat less than the 10–20 nm Soret red-shift that Hendrickson *et al.* reported is typical for this reduction.[19]

An alternative explanation for the red-shift of the Soret peak of supported FeTPFPP and FeTDCPP is that there is an interaction between the metalloporphyrin and the support which reduces the dihedral angle between the porphyrin plane and the *meso*-aryl groups. This would result in an increased conjugation and a red-shift of the Soret peak. Such a proposal has been made previously by Mansuy and his co-workers[12b] to account for the red-shift of the Soret peak of 4-*N*-methylpyridyl substituted metalloporphyrins supported on a clay. However, although this is possible with FeTPFPP, the 2,6-dichlorophenyl groups on FeTDCPP are considerably more hindered than 4-*N*-methylpyridyl and should resist this change in conformation. Furthermore the ligand with the co-ordinatively bound catalyst anchors the metalloporphyrin at a distance from the support surface so that it is unlikely that this is the cause of the red-shift observed in the present study.

To confirm the presence of iron(II) porphyrin, we examined the UV–VIS spectrum of a dichloromethane suspension of SiPy–FeTDCPP following saturation with carbon monoxide. This showed a broadened Soret peak with a shoulder to longer wavelength. Furthermore when the suspension was allowed to settle, the solution had an absorption at 446 nm. Carbon monoxide complexes of iron(II) porphyrins have a characteristic Soret peak typically between 440 and 450 nm.[20] This result indicates that carbon monoxide, a strong field ligand, is able to compete with the pyridine groups and remove the Fe^{II}TDCPP from the support.

The Soret λ_{max} values of the iron porphyrins on PSIm indicate that both are iron(II) species and, by analogy with the PVP bound catalysts, these are likely to be *bis*-ligated complexes. This shows that PSIm is a better reducing agent than *N*-benzylimidazole since the latter does not reduce Fe^{III}TDCPP and only partially reduces Fe^{III}TPFPP. It is possible that the greater reducing power of PSIm arises from binding the imidazole groups to the surface of the polymer which effectively increases their local concentration compared to those in the reactions in solution.

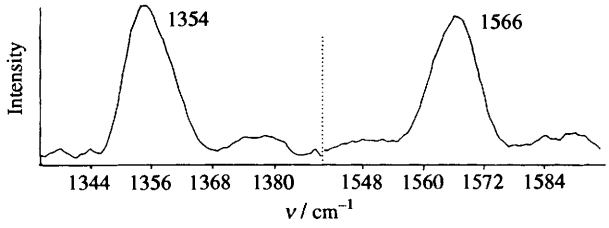

Fig. 6 Resonance Raman spectrum of PSIm–FeTPFPP in the regions 1330–1390 and 1540–1600 cm^{-1}

The conclusions from the UV–VIS spectra of the iron porphyrins ligated to SiIm are less clear cut. With SiIm–FeTPFPP the assignment of the oxidation state of the iron is ambiguous since the λ_{max} of the Soret peak lies midway between those of iron(III) and iron(II) TPFPP. Resonance Raman spectroscopy suggests that this is a mixture of iron(III) and iron(II) species (see below). The position of Soret peak of SiIm–FeTDCPP indicates reduction to iron(II) has occurred even though Fe^{III}TDCPP is less readily reduced than Fe^{III}TPFPP and consequently an iron(III) species would be expected. The oxidation state was confirmed as iron(III) by bubbling CO through a $CHCl_3$ suspension of SiIm–FeTPFPP: UV–VIS spectroscopy showed no evidence of an iron(II) porphyrin–CO complex being present.

Resonance Raman spectroscopy of supported iron porphyrins

The resonance Raman spectra of five of the supported catalysts were recorded in the regions 1300–1400 and 1500–1600 cm^{-1} to measure the wavenumbers of the A and D spin and oxidation state marker bands[6] (Table 3 and see for example Fig. 6). Interestingly neither catalyst bound to SiIm gave a detectable peak in the region of band D (1500–1600 cm^{-1}) and SiIm–FeTPFPP gave two peaks in the band A region (1300–1400 cm^{-1}). The Raman spectra of some homogeneous models are also reported to provide comparative data (Table 5).

Resonance Raman spectroscopy has been used to obtain information on the spin and oxidation states of both natural and synthetic metalloporphyrins.[6] In particular there is a large body of data on FeTPP complexes:[21] the wavenumber ranges of the A and D bands of these are reported in Table 6. Almost all of the band wavenumbers of the solution spectra in the present study lie within the ranges quoted for FeTPP complexes. The most notable exception is the high-spin complex of Fe^{III}TPFPP. This can be attributed to the electron withdrawing pentafluorophenyl groups; a similar effect has been observed previously for FeT4MPyP complexes.[22] It is apparent that band A is a good indicator of the oxidation and band D of the spin state.

Comparison of the Raman data from the supported iron porphyrins (Table 3) with those in Tables 5 and 6 allows an assignment of the spin and oxidation states of the former. The complexes on the flexible organic polymers, PSIm–FeTPFPP and PVP–FeTDCPP, have band A values at 1354 and 1353 cm^{-1} respectively indicating that the iron in both is in the +2 oxidation state. However, the band D wavenumbers of the two materials are significantly different at 1566 and 1558 cm^{-1} respectively. The former suggests a low-spin species is present. However, for PVP–FeTDCPP the assignment of the band D is unclear. It lies within the wide range of values for low-spin iron(II) porphyrins in Tables 5 and 6 although it is closer to that of high-spin FeTDCPP than to those of the low-spin complexes of this iron porphyrin. Taking into account the properties[10a] and UV–VIS spectra of the polymer supported metalloporphyrins, we conclude that both are probably *bis*-ligated, low-spin iron(II) species.

Table 5 Resonance Raman data for iron porphyrins in solution

Iron porphyrin	Ligand	Solvent	Spin state[a]	Oxidation state	Band A/cm^{-1}	Band D/cm^{-1}
FeTPFPP	Cl	PhH	HS	+3	1368	1557
FeTDCPP	Cl	$CHCl_3$	HS	+3	1362	1559
FeTDCPP	$(NBzIm)_2$[b]	$CHCl_3$	LS	+3	1368	1567
FeTPFPP	$(NBzIm)_2$[b]	PhH	LS	+2	1358	1567
FeTPFPP	$(NH_2NH_2)_2$	PhH	LS	+2	1360	1565
FeTDCPP	$(NH_2NH_2)_2$	$CHCl_3$	LS	+2	1354	1564
FeTDCPP	$(4MePy)_2$[c]	$CHCl_3$	LS	+2	1360	1564
FeTDCPP	$(NMeIm)_2$[d]	$CHCl_3$	LS	+2	1357	1566
FeMesoP[e,f]	(2MeIm)[g]	CH_2Cl_2	HS	+2	1359	1558
FeHb[f,h]	Protein	H_2O	HS	+2	1358	1552
FeHRP[f,i]	Protein	H_2O	HS	+2	1358	1553

[a] HS, high spin and LS, low spin. [b] *N*-benzylimidazole. [c] 4-Methylpyridine. [d] *N*-Methylimidazole. [e] Iron mesoporphyrin. [f] Ref. 16. [g] 2-Methylimidazole. [h] Haemoglobin. [i] Horseradish peroxidase.

Table 6 Resonance Raman wavenumber ranges for FeTPP complex[21]

Spin state[a]	Oxidation state	Band A/cm^{-1}	Band D/cm^{-1}
HS	+3	1356–1363	1541–1554
HS	+2	1341–1345	1538–1542
LS	+3	1365–1370	1561–1568
LS	+2	1355–1369	1560–1572

[a] HS, high spin and LS, low spin.

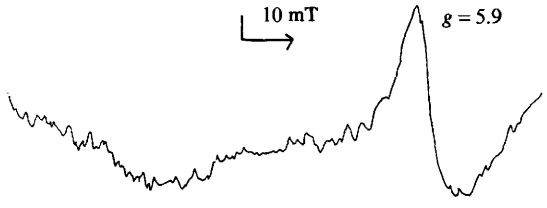

Fig. 7 EPR spectrum of SiIm–FeTDCPP at 120 K

Although neither of the iron porphyrins supported on SiIm gave a detectable band D (spin state marker), the band A data are consistent with SiIm–FeTDCPP being a high-spin iron(III) species (1362 cm^{-1}) and SiIm–FeTPFPP being a mixture of high-spin iron(III) and iron(II) complexes [1364 (major) and 1345 (minor) cm^{-1}]. The high-spin assignments are readily understood since the rigid inorganic support would only allow monoligation of the supported-imidazole to the metalloporphyrin and would result in the displacement of the iron from the plane of the porphyrin ring. Partial reduction of the iron in SiIm–FeTPFPP is favoured by the electron-withdrawing pentafluorophenyl groups, as discussed above.

The assignment of the spin and oxidation state of SiPy–FeTDCPP is not so clear-cut. Band A at 1353 cm^{-1} is particularly low for an iron(III) complex and suggests an iron(II) species [*cf.* FeTDCPP$(NH_2NH_2)_2$ 1354 cm^{-1}]. Band D (1555 cm^{-1}), however, does not lie in the expected region for low-spin iron [1564 cm^{-1} for both Fe^{II}TDCPP(4-MePy)$_2$ and Fe^{II}TDCPP$(NH_2NH_2)_2$] instead it correlates well with the high-spin marker band of Fe^{III}TDCPP (1559 cm^{-1}). On the basis of these data we conclude that SiPy–FeTDCPP is a high-spin iron(II) species, unlike SiIm–FeTDCPP which is high-spin iron(III) and SiIm–FeTPFPP which is a mixture of high-spin iron(III) and iron(II) species. This is consistent with monoligation to the rigid support and the greater tendency of 4-methylpyridyl than *N*-methylimidazole to act as a reducing agent for iron(III) tetraarylporphyrins.

EPR Spectroscopy of supported iron porphyrins

FeTDCPP in solution and supported on SiIm and SiPy was studied further using EPR spectroscopy. The first two catalysts gave the characteristic signals of a high spin iron(III) porphyrin, $g_\perp$ values 5.68 and 5.9,[2,23] respectively (Fig. 7) in agreement with the resonance Raman and UV–VIS results. In contrast, SiPy–FeTDCPP gave a very broad EPR signal. If as suggested above SiPy–FeTDCPP is a high-spin iron(II) complex, it will be a d^6 $S = 2$ species. EPR spectra of $S = 2$ complexes are rare[24] and if the zero field splitting is large enough then the signal may be almost completely broadened away.[25]

Conclusions

In the co-ordination of iron(III) porphyrins to the supported nitrogen ligands examined in this study:

(*i*) the support backbone determines the spin state of the iron porphyrins; flexible organic polymer supports lead to low spin *bis*-ligated complexes whereas rigid modified silicas form high spin species;

(*ii*) the nitrogen ligand can bring about reduction of the bound iron(III) porphyrin; 4-substituted pyridine favours reduction compared with the *N*-substituted imidazoles;

(*iii*) electron-withdrawing groups on the porphyrin ligand stabilise iron(II) relative to iron(III).

Experimental

Materials

Unless otherwise stated the reagents were commercially available. The preparation of the iron(III) porphyrins and of the polymer and modified silica supported catalysts have been reported previously.[10]

Methods

IR spectra as KBr discs or KBr powders were recorded using a Perkin-Elmer 1720 FT spectrometer.

CPMAS ^{13}C NMR spectra were measured on a Bruker MSL 300 spectrometer (300 MHz) using adamantane as a reference.

Electron micrographs of supports and supported catalysts were obtained using a Hitachi Model S-2400 scanning electron microscope.

UV–VIS spectra of dichloromethane suspensions and Nujol mulls were recorded using a Hewlett Packard 8452A Diode array spectrometer. Diffuse reflectance UV–VIS spectra were recorded by Dr H. Herman, BP Chemicals, Sunbury, using a Perkin-Elmer Lambda 9 UV–VIS spectrometer fitted with a powder attachment.

EPR spectra were recorded with a Bruker ESP 300 spectrometer, fitted with an X-band klystron, 100 kHz modulation and ESP 1600 Data system. Liquid nitrogen was

used to cool the sample cavity and the low temperatures (120 K) were maintained using a Bruker ER 4111 VT variable temperature unit.

Resonance Raman spectra of solutions in a spinning quartz cell were obtained with a Jobin-Yvon HR640 double spectrograph and a Wright Instruments liquid nitrogen cooled camera, with a krypton ion laser functioning at an excitation wavelength of 406.7 nm or an argon ion laser at 457.9 nm. Solid samples of supported iron porphyrins were prepared by grinding up supported catalyst with 10% by volume of potassium bromide. These samples were compressed into a metal disc under *ca.* 5 tonne pressure and the disc was spun during acquisition of the spectra.

Acknowledgements

We thank Dr C. Lefley for running the resonance Raman spectra, Dr J. N. Moore for helpful discussions in connection with these spectra and the SERC and BP Chemicals, Hull for a CASE research studentship.

References

1 J. R. Lindsay Smith, in *Metalloporphyrins in Catalytic Oxidations*, ed. R. A. Sheldon, Marcel Dekker, New York, 1994, ch. 11.
2 G. Palmer, in *Iron Porphyrins*, Part 2, ed. A. B. P. Lever and H. B. Gray, Addison-Wesley, 1983, p. 43.
3 J. O. Alben, in *The Porphyrins*, ed. D. Dolphin, Academic Press, New York, 1978, vol. 3, part A, p. 323.
4 P. G. Debrunner, in *Iron Porphyrins*, Part 3, ed. A. B. P. Lever and H. B. Gray, VCH, 1989, p. 137.
5 H. M. Goff, in *Iron Porphyrins*, Part 1, ed. A. B. P. Lever and H. B. Gray, Addison-Wesley, 1983, p. 237.
6 T. G. Spiro, in *Iron Porphyrins*, Part 2, eds. A. B. P. Lever and H. B. Gray, Adison-Wesley, 1983, p. 89.
7 J. E. Falk, in *Porphyrins and Metalloporphyrins*, Elsevier, London, 1964, vol. 2.
8 J. E. Penner-Hahn and K. O. Hodgson, in *Iron Porphyrins*, Part 3, ed. A. B. P. Lever and H. B. Gray, VCH, 1989, p. 235.
9 (*a*) D. G. Davis, in *The Porphyrins*, ed. D. Dolphin, Academic Press, New York, 1978, vol. 5, p. 127; (*b*) K. M. Kadish, in *Iron Porphyrins*, Part 2, ed. A. B. P. Lever and H. B. Gray, Addison-Wesley, 1983, p. 161.
10 (*a*) P. R. Cooke and J. R. Lindsay Smith, *J. Chem. Soc., Perkin Trans. 1*, 1994, 1913; (*b*) C. Gilmartin and J. R. Lindsay Smith, *J. Chem. Soc., Perkin Trans. 2*, 1995, 243.
11 H. L. Retcofsky and R. A. Friedel, *J. Phys. Chem.*, 1967, **71**, 359.
12 (*a*) S. S. Cady and T. J. Pinnavaia, *Inorg. Chem.*, 1978, **17**, 1501; (*b*) L. Barloy, J.-P. Lallier, P. Battioni, D. Mansuy, Y. Piffard, M. Tournoux, J. B. Valin and W. Jones, *New J. Chem.*, 1992, **16**, 71.
13 K. Hatano, M. K. Safo, F. A. Walker and W. R. Scheidt, *Inorg. Chem.*, 1991, **30**, 1643.
14 (*a*) C. L. Coyle, P. A. Rafson and E. H. Abbot, *Inorg. Chem.*, 1973, **12**, 2007; (*b*) F. A. Walker, M. W. Lo and M. T. Ree, *J. Am. Chem. Soc.*, 1976, **98**, 5552; (*c*) J. D. Satterlee, G. N. La Mar and J. S. Frye, *J. Am. Chem. Soc.*, 1976, **98**, 7275; (*d*) F. A. Walker, J. A. Barry, V. L. Balke, G. A. McDermott, M. Z. Wu and P. F. Linde, *Adv. Chem. Ser.*, 1982, **201**, 377; (*e*) V. L. Balke, F. A. Walker and J. T. West, *J. Am. Chem. Soc.*, 1985, **107**, 1226.
15 (*a*) H. Kobayashi and Y. Yanagawa, *Bull. Chem. Soc. Jpn.*, 1972, **45**, 450; (*b*) T. Yoshimura, H. Toi, S. Inoba and H. Ogoshi, *Bull. Chem. Soc. Jpn.*, 1992, **65**, 1915.
16 T. G. Spiro and J. M. Burke, *J. Am. Chem. Soc.*, 1976, **98**, 5482.
17 P. R. Cooke, D.Phil. Thesis, University of York, 1993.
18 (*a*) L. M. Epstein, D. K. Straub and C. Maricondi, *Inorg. Chem.*, 1967, **6**, 1720; (*b*) J. Del Gaudio and G. N. La Mar, *J. Am. Chem. Soc.*, 1978, **100**, 1112; (*c*) G. S. Srivasta and D. T. Sawyer, *Inorg. Chem.*, 1985, **24**, 1732; (*d*) C. E. Castro, M. Jarvin, W. Yokoyama and R. Wade, *J. Am. Chem. Soc.*, 1986, **108**, 4179; (*e*) T. Yoshimura, H. Toi, S. Inoba and H. Ogoshi, *Inorg. Chem.*, 1991, **34**, 4315.
19 D. N. Hendrikson, M. G. Kinnaird and K. S. Suslick, *J. Am. Chem. Soc.*, 1987, **109**, 1243.
20 P. R. Ortiz de Montellano, in *Cytochrome P450, Structure, Mechanism and Biochemistry*, ed. P. R. Ortiz de Montellano, Plenum Press, New York, 1986, p. 275.
21 (**a**) J. M. Burke, J. R. Kinkaid, S. Peters, R. R. Gagne, J. P. Collman and T. G. Spiro, *J. Am. Chem. Soc.*, 1978, **100**, 6083; (*b*) G. Chottard, P. Battioni, J.-P. Battioni, M. Lange and D. Mansuy, *Inorg. Chem.*, 1981, **20**, 1718; (*c*) P. Stein, A. Ulman and T. G. Spiro, *J. Phys. Chem.*, 1984, **88**, 369; (*d*) L. M. Proniewicz, K. Bajdor and K. Nakamoto, *J. Phys. Chem.*, 1986, **90**, 1760; (*e*) N. Parthasarathi, C. Hansen, S. Yamaguchi and T. G. Spiro, *J. Am. Chem. Soc.*, 1987, **109**, 3865.
22 S. E. J. Bell, R. E. Hester, J. N. Hill, D. R. Shawcross, J. R. Lindsay Smith, *J. Chem. Soc., Faraday Trans.*, 1990, **86**, 4017.
23 K. R. Rodgers, R. A. Reed, Y. O. Su and T. G. Spiro, *Inorg. Chem.*, 1992, **31**, 2688.
24 M. Symons, *Chemical and Biochemical Aspects of Electron Spin Resonance Spectroscopy*, Van Norstrand Reinhold, 1978, p. 2139; J. R. Pilbrow, *Transition Ion Electron Paramagnetic Resonance*, Oxford, 1990, p. 499.
25 A. Carrington and A. D. McLachlan, *Introduction to Magnetic Resonance*, Wiley, Chichester, 1979, p. 164; J. R. Pilbrow, *Transition Ion Electron Paramagnetic Resonance*, Oxford, 1990, p. 135.

Paper 5/02017D
Received 30*th March* 1995
Accepted 11*th May* 1995